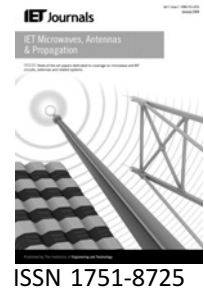


Published in IET Microwaves, Antennas & Propagation
 Received on 4th September 2008
 Revised on 22nd January 2009
 doi: 10.1049/iet-map.2008.0301



Study of a microwave ferrite resonator antenna, based on a ferrimagnetic composite $(\text{Gd}_3\text{Fe}_5\text{O}_{12})\text{GdIG}_x-(\text{Y}_3\text{Fe}_5\text{O}_{12})\text{YIG}_{1-x}$

P.B.A. Fechine¹ H.H.B. Rocha² R.S.T. Moretzsohn²
 J.C. Denardin³ R. Lavín⁴ A.S.B. Sombra²

¹Departamento de Química Analítica e Físico-Química, Universidade Federal do Ceará – UFC, Campus do Pici, CP 12100, CEP, 60451-970 Fortaleza – CE, Brazil

²Laboratório de Telecomunicações e Ciência e Engenharia dos Materiais - (LOCEM), Departamento de Física, Universidade Federal do Ceará, Fortaleza, Ceará, Brazil

³Departamento de Física, Universidad de Santiago de Chile, USACH, Avenida Ecuador 3493, Santiago, Chile

⁴Facultad de Ingeniería, Universidad Diego Portales, Ejército 441, Santiago, Chile
 E-mail: fechine@ufc.br

Abstract: The authors report a study on microwave properties of a ferrimagnetic ceramic composite $(\text{Gd}_3\text{Fe}_5\text{O}_{12})\text{GdIG}_x-(\text{Y}_3\text{Fe}_5\text{O}_{12})\text{YIG}_{1-x}$. The magnetic and dielectric measurements at microwave frequency were made through the Hakki–Coleman’s procedure and through the excitation of a cylindrical ferrite resonator antenna (FRA). The hysteresis loops of the $\text{GdIG}_x\text{YIG}_{1-x}$ ferrimagnetic composite were obtained. The numerical simulation study was performed using Ansoft’s High Frequency Structure Simulator (HFSSTM) software. The agreement between the experimental data and the simulated results is very good. These results demonstrated that, by varying the material composition of the resonator, ferrimagnetic composite $\text{GdIG}_x\text{YIG}_{1-x}$ could operate as a magneto-dielectric antenna with bandwidth in the range of 7.5–11% and in the frequency range of 4.4–5.3 GHz. Additionally, all FRAs presented a low negative value of τ_f , which indicates suitability for microwave applications such as mobile communication systems or satellite broadcast systems.

1 Introduction

The dielectric resonator (DR) has various shapes: cylindrical, rectangular, hemispherical, low profile circular disk, low profile triangular, spherical cap etc. [1, 2]. It requires a material of relative dielectric permittivity (ϵ_r') sufficiently high for a standing electromagnetic wave to be sustained within its volume because of total internal reflection at the dielectric–air interface [1]. The application of these components as antennas in microwave and millimetre band has been extensively studied [3], as they have advantages such as light weight, low cost, small size, low profile, high radiation efficiency, large bandwidth and ease of integration with other active or passive microwave integrated circuit components.

In essence, an antenna is a component that converts wave propagation on a transmission line to a plane wave propagating in free space (transmission), or vice versa (reception) [4]. A dielectric resonator antenna (DRA) is a resonant antenna, fabricated from low loss microwave dielectric material, where the resonant frequency is predominantly a function of size, shape and material permittivity. The DR used for antenna applications has a high dielectric constant, typically with ϵ_r' ranging from 10 to 100. The mode of operation depends on the geometry of the resonator and on the required radiation patterns [5].

DRA offers several advantages compared to conventional metallic antennas such as monopoles or helix. They are less

easily broken off, easily styled into products that are more fashionable to today's consumers and generally reduce power absorption by the head [2]. As compared to the microstrip antenna, the DRA has a much wider impedance bandwidth ($\sim 10\%$ for $\epsilon'_r \sim 10$). This is because the microstrip antenna radiates only through two narrow radiation slots, whereas the DRA radiates through the whole DRA surface except the grounded part [2].

Electronic ceramics [6–9] have many applications in microwave communication systems [10–12], where dielectrics are used both for elements in microwave integrated circuits and for the substrates on which circuit elements are fabricated. The ferrites are a group of electronic ceramics, which are used in microwave components like circulators and isolators. Microwave integrated circuits offer size and cost advantages compared to discrete waveguide components [13]. Rapid growth in ferrite usage was propagated by a trend towards higher frequencies of operation in telecommunications and power electronic applications. Major applications of ferrites include magnetic cores for inductors and transformers (for spinels, up to 200 MHz; for planar hexaferrites from 200 to 800 MHz), permanent magnets (for uniaxial hexaferrites), microwave devices (spinel, garnets), magneto-optic devices (garnets) and electro-mechanical transducers (spinel) [14]. A high resistivity is desired for most of these applications in order to minimise eddy currents or dielectric loss.

A combined study of both the crystal structure and the electrical properties of new compounds and solid solutions is necessary for the development of new ceramic materials. A refinement of new stoichiometric compositions and homogeneity regions is leading the research for new materials [15]. Therefore synthetic ferrites have been formulated to obtain specific magnetic properties in a wide variety of applications.

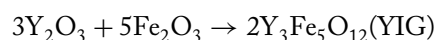
In this paper, we prepared two different garnets structured to make a ferrimagnetic composite to use as a ferrite resonator antenna (FRA). We studied the magnetic characteristics of the composites and dielectric properties, using Hakki and Coleman's experiment. A numerical study was also performed to support the experimental measurements of the FRA using the High Frequency Structure Simulator (HFSS) software.

2 Experimental methods

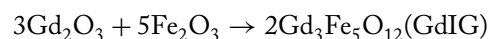
2.1 Preparation of ferrimagnetic materials

Stoichiometric amounts of Y_2O_3 (99.99%, Aldrich) and Fe_2O_3 (99.00%, Aldrich) were used in YIG preparation. The material was ground on a Fritsch Pulverisette 6 planetary mill in sealed stainless-steel vials (221.69 cm^3) and balls ($\varnothing 10 \text{ mm}$) under air in weight ratio 1/9 (wt. of mixture powder/wt. of balls). Mechanical alloying was

performed for 1 h of milling with 370 rpm. After this, the powder was submitted to calcination in air at 1150°C for 5 h. The reaction occurring during calcination can be summarised as



Gd_2O_3 (99.9%, Fluka) and Fe_2O_3 (99.0%, Aldrich) powder mixture had the same treatment utilised by YIG starting materials. However, this powder mixture was submitted to calcination in air at 1250°C for 5 h. The reaction occurring during calcination can be summarised as



A total of 5% of a mixture [71.82 mmol of B_2O_3 (99.0%, Aldrich) and 10.73 mmol of Bi_2O_3 (99.9%, Aldrich)] homogenised for 10 h of milling was added in the calcined powder as a sintering aid. Also, 5% of the organic material (Glycerin, 99.5% – O Moreira & Cia Ltda) was added to improve plastic features. These mixtures were uniaxially pressed into pellets at approximately 111 MPa. Then, green compacts were sintered for 12 h at 1200°C under air. Thus we prepared five DRs with different composition. The $GdIG_XYIG_{1-X}$ nomenclature was utilised to differentiate the ferrimagnetic composites, where X (1, 0.75, 0.5, 0.25 and 0) was given in wt%.

2.2 Magnetic measurements

The magnetisation measurements were performed at room temperature with a home-made vibrating sample magnetometer (VSM). The VSM has been previously calibrated using a pure Ni wire, and after measuring the mass of each sample the magnetisation was given in emu/g.

2.3 Hakki and Coleman's experiment

The dielectric properties at the microwave range were obtained from the sizes of the samples and the value of the resonant frequency, using the Hakki and Coleman's dielectric resonant TE_{011} and $TE_{01\delta}$ methods. An HP 8716ET network analyser was employed to make the measurements [16–18]. From the resonant frequency of the TE_{011} mode, the dielectric permittivity ϵ'_r and loss $\text{tg } \delta_E$ were obtained (see Table 1). The values obtained in this experiment were used as a guide in the numerical simulation of the antennas, with the assumption that the variation of ϵ'_r with the frequency is not big between 7 GHz (mean resonant frequency of the Hakki–Coleman experiment) and 4 GHz (mean resonant frequency of the antenna experiment).

The $TE_{01\delta}$ mode allows accurate measurement of the dielectric constant at both high and low temperatures. The Hakki–Coleman DR method was employed to characterise the temperature coefficient of resonance frequency (τ_f) measurements. Experimentally, τ_f is measured by following

Table 1 Microwave measurements obtained from Hakki–Coleman procedure; thickness (e), diameter (D), dielectric resonant TE_{011} (f_r), dielectric constant (ϵ'_r), dielectric loss ($\text{tg } \delta_E$) and quality factor (Q_u)

Sample	e (mm)	D (mm)	φ (g/cm ³)	φ_r (%)	f_r (GHz)	ϵ'_r	$\text{tg } \delta_E$	Q_u
GdIG	7.608	15.559	5.89	91.23	7.135	14.473	0.012	83.01
GdIG _{0.75} YIG _{0.25}	7.737	15.937	5.71	93.19	7.539	12.439	0.004	251.87
GdIG _{0.5} YIG _{0.5}	8.414	16.262	5.29	88.96	7.566	10.987	0.003	339.00
GdIG _{0.25} YIG _{0.75}	9.044	16.551	5.18	90.62	7.624	9.795	0.002	464.13
YIG	9.414	16.572	4.86	88.27	7.688	9.189	0.001	668.99

φ and φ_r represent density and relative density measurements by Archimedes' method, respectively

the drift in the $TE_{01\delta}$ resonant peaks frequencies as the temperature is slowly varied from $T_i = 25^\circ\text{C}$ to $T_f = 100^\circ\text{C}$ ($\Delta T = T_f - T_i = 75^\circ\text{C}$). Then, τ_f is obtained by taking the slope of the graph of $\Delta f/f_{25}$ against $1/\Delta T$, whose mathematical relationship is [19]

$$\tau_f = \frac{\Delta f}{f_{25}} \frac{1}{\Delta T} (\text{ppm}/^\circ\text{C}) \quad (1)$$

where Δf is the difference between the final and initial frequencies, ΔT is the difference between the final and initial temperatures and f_{25} is the resonant frequency in the arbitrary standard temperature (25°C). Usually, τ_f is scaled up by 10^6 and reported in parts per million per degree ($\text{ppm}/^\circ\text{C}$). It is relevant to mention that an adequate balance of dielectric properties as low dielectric permittivity ($\epsilon'_r < 40$), low dielectric loss ($\tan \delta < 5 \times 10^{-3}$) and near-zero temperature coefficient (τ_f) of resonant frequency are requirements, respectively, for good enhanced radiation properties, stable resonant frequency and thermal stability of microwave components.

2.4 Antenna experiment numerical simulation procedures

The ferrite resonators were excited by a wire antenna protruding above a ground plane [20]. The configuration of the cylindrical FRAs is shown in Fig. 1. The FRA is placed above a conducting ground plane (the ground plane is made of copper, with dimensions $35.5 \text{ cm} \times 30 \text{ cm} \times 2.14 \text{ mm}$) and excited by a coaxial probe ($L = 9 \text{ mm}$). The coaxial probe goes through the ground plane and is connected to an SMA connector. In Fig. 1, the cylindrical FRA has a radius a , height h and dielectric permittivity ϵ'_r . The probe is located on the x -axis at $x = a$ and $\varphi = 0$.

The cylindrical FRA works at the $HE_{11\delta}$ mode, whose resonant frequency f_r can be approximated [21] by

$$f_r = \frac{2.997 \times 10^8}{2\pi \sqrt{\mu_r \epsilon'_r}} \sqrt{\left(\frac{1.841}{a}\right)^2 + \left(\frac{\pi}{2h}\right)^2} \quad (2)$$

Equation (2) is obtained with the hypothesis that the lateral

and upper surfaces of the ferrite resonator are perfectly magnetic conductors (PMC). Because this assumption is verified only for infinite permittivity, (2) is only an approximation that leads to errors of some 10%.

It is important to note that both experimental and simulation results show a great variability of the results depending on the depth of the probe into the FRA. This problem, that finds its origin in the presence of an air gap between the FR and the metallic conductors, has been thoroughly studied by Junker *et al.* [22, 23]. To illustrate the effect, we define in Fig. 1 two parameters associated with the air gap e_1 between the dielectric and the probe, and e_2 between the dielectric and the ground plane.

The simulations were carried out using Ansoft's HFSS, a software package based on the finite-element method (FEM). An objective of this study involves a numerical validation of the experimental setup. As a first advantage, it is possible to investigate the influence of the probe on the resonant frequencies. Besides, the high sensitivity of the results in the function of the air gap can be confirmed.

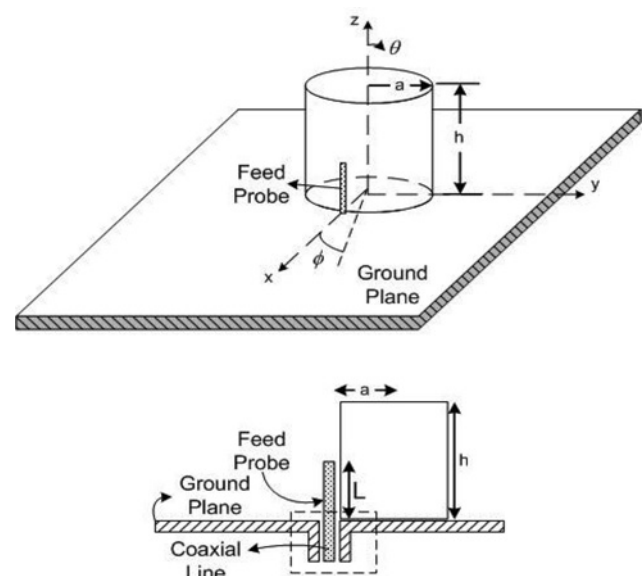


Figure 1 Geometry of the cylindrical FRA

As a final point, HFSS software provides the radiation patterns of the antennas under investigation.

3 Results and discussion

Firstly, we studied the DC magnetic features of the $\text{GdIG}_X\text{YIG}_{1-X}$ composite. Fig. 2 shows the variation in magnetisation, M , against bias field, H , of the samples. The shape of the hysteresis loops obtained from this experiment was typical of soft ferrites characteristic of their values of coercive field (H_C), remanent (M_r) and saturation (M_S) magnetisation. One can notice a decrease of the M_S as a function of GdIG concentration, and this factor may be of importance with regard to the properties of the FRAs. Saturation magnetisation of YIG was observed at 21.72 emu/g, which is reasonably closer to the bulk saturation magnetisation of YIG (which is around 26 emu/g) [24].

The dielectric properties of the $\text{GdIG}_X\text{YIG}_{1-X}$ composite were obtained from Hakki–Coleman's procedure and are presented in Table 1. Values of resonant frequency (f_r) were attributed to TE_{011} mode, where we assumed $\mu'_r = 1$. We observed that ϵ'_r and $\text{tg } \delta_E$ values increased with the increase in the X value (GdIG presence in the composite), whereas the quality factor unload (Q_u) decreased. This happened because Gd has a higher density than the Y atom, that is the density of the GdIG structure is higher than YIG. In Table 1 one can also observe the values of density (ρ) and relative density (ρ_r) of the composites, both were measured by Archimedes' method. The ρ values had approximately a linear behaviour.

The increase of X [presence of GdIG composition (wt%) in the composites] in the cylindrical FRA moves the resonant frequency of the $\text{HE}_{11\delta}$ mode (f_0) to lower frequencies, as shown in Fig. 3. This was caused by a consequential increase

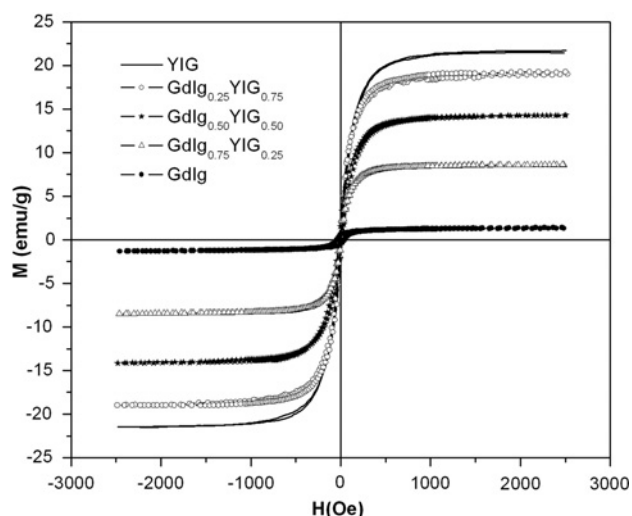


Figure 2 VSM measurements of magnetisation, M (emu/g), as a function of magnetic field strength, H (Oe), of the $\text{GdIG}_X\text{YIG}_{1-X}$ composite at room temperature

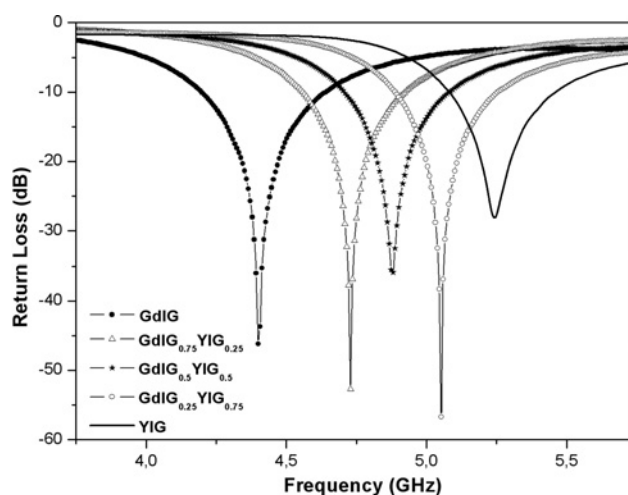


Figure 3 Return losses measurement of $\text{GdIG}_X\text{YIG}_{1-X}$ composite as FRA

of ϵ'_r as a function of GdIG composition, see equation (2). These results showed that it is possible to develop an antenna that operates in the frequency range of 4.4–5.3 GHz, controlling only the composition of the resonator. Therefore f_0 and ϵ'_r , as well as M_S , depend on the GdIG concentration in the composite and had a linear behaviour, as shown in Fig. 4.

Table 2 shows the experimental and simulated values of f_0 to the FRAs. The error between both, for all samples, was acceptable and for the case of GdIG was virtually non-existent. The bandwidth of the antennas, measured in -10 dB, was higher than 7%. The maximum bandwidth was obtained for the $\text{GdIG}_{0.5}\text{YIG}_{0.5}$ resonator (see Table 2). The bandwidth of the antenna is mainly influenced by the permittivity of the material [25]. The simulated results were also acceptable because of the small error. In Fig. 5 one can observe an example of the good agreement between simulation and experimental data of the return loss (S_{11}) for $\text{GdIG}_{0.75}\text{YIG}_{0.25}$ composite, where the return loss had the value of -55 dB at the resonance frequency.

In Table 3 we present some magnetic and dielectric results for the FRAs. The values for ϵ'_r and μ'_r were obtained from the numerical simulation. They also depend on the frequency of resonance (f_0) of the antenna. The μ'_r for the GdIG resonator was 1.10; however, the increase of YIG (0.35) composition (wt%) is leading to a decrease in this value. The dielectric ($\text{tg } \delta_E$) and magnetic loss ($\text{tg } \delta_M$) measurements presented values in the range of 10^{-3} – 10^{-4} , which are good results for an antenna application, see Table 3. The maximum resistance of the resonant frequency of each FRA is also indicated in the same table. For FRAs, these experimental values ranged from 105.51 Ω (GdIG) to 171.23 Ω (YIG), that is the increase of the YIG composition in FRA causes increase of resonant resistance. The simulated results were found to be in good agreement with the experimental values.

The complex S_{11} is reported in the Smith chart of $\text{GdIG}_{0.75}\text{YIG}_{0.25}$ FRA to have a more precise idea of the

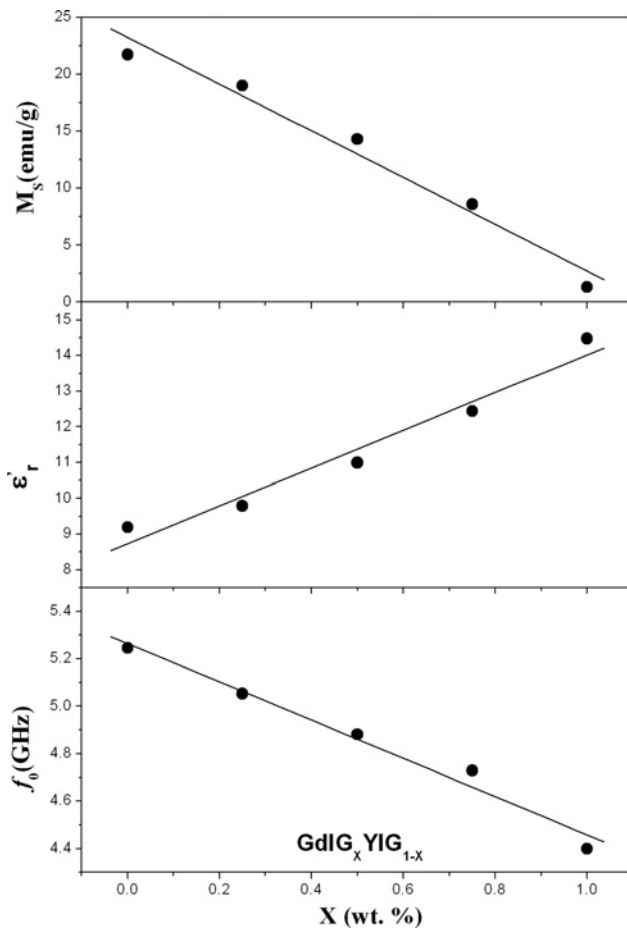


Figure 4 f_0 , ϵ_r' and M_S values as a function of GdIG composition (wt%)

antenna behaviour (see Fig. 6). The agreement between the experimental and the theoretical values is good. Using the data plotted on a Smith chart, it was possible to find the resonant frequency of the $\text{HE}_{11\delta}$ mode, the values of the resistances being close to 50Ω . These values were found in the minimum of the return loss (f_0) and their experimental and simulated results are presented in Table 3. A good approximation was observed for both because of the matching impedances. In Fig. 7 one can see that the input impedance (Z), composed of real (Z') and imaginary (Z'') parts, presents

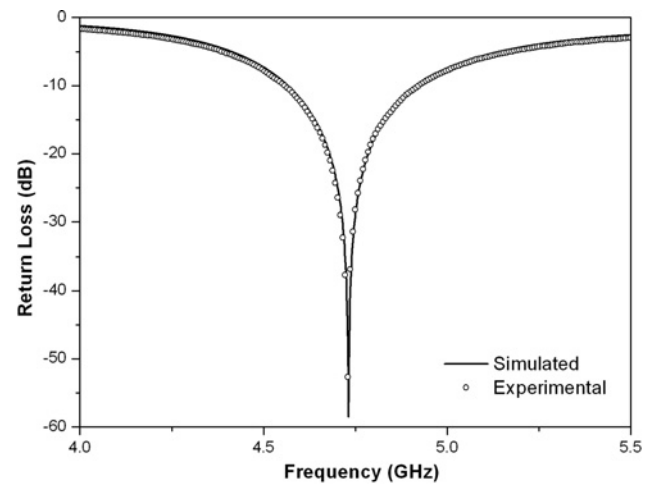


Figure 5 Experimental (measured) and theoretical (simulated) return losses of GdIG_{0.75}YIG_{0.25} FRA

a frequency response because of the resonant response of each mode. At the peak of real part of impedance, the resistance shows a maximum. Thus, a successful agreement was obtained between simulation from HFSS modelling and experimental methodology, which demonstrates the effectiveness of modelling of the FRAs using Ansoft's HFSS.

Fig. 8 shows the simulated radiation pattern of E_θ and E_ϕ planes at resonant frequency of the GdIG_{0.75}YIG_{0.25}. On an infinite ground plane, the antenna pattern would be omnidirectional with a beam peak at the horizon ($\theta = 90^\circ$) similar to that of a monopole antenna [26]. Symmetry of the field patterns is related to the feed probe location at $\phi = 0^\circ$. One can notice two symmetric lobes for $\phi = 90$ and 0° at the E_θ plane. This shows an omni-directional pattern for both, as was foreseen.

Three FRAs (GdIG, GdIG_{0.5}YIG_{0.5} and YIG) were selected for measurement of the microwave temperature coefficient of resonant frequency (τ_f). Fig. 9 shows the linear fit with the experimental points used to calculate τ_f , see (1). τ_f from GdIG was $-388.45 \text{ ppm}/^\circ\text{C}$ and this value was higher than GdIG_{0.5}YIG_{0.5} ($-225.24 \text{ ppm}/^\circ\text{C}$)

Table 2 Antenna resonant frequency (f_0) and bandwidth of the $\text{HE}_{11\delta}$ mode with experimental (Exp.) and simulated (Sim.) values

Sample	f_0 (GHz)			Bandwidth (%)		
	Exp.	Sim.	Error (%)	Exp.	Sim.	Error (%)
GdIG	4.399	4.399	0	11.64	8.02	3.62
GdIG _{0.75} YIG _{0.25}	4.729	4.731	4.23×10^{-2}	7.61	7.46	0.15
GdIG _{0.5} YIG _{0.5}	4.881	4.87	0.22	7.61	11.17	-3.56
GdIG _{0.25} YIG _{0.75}	5.052	-	-	7.08	-	-
YIG	5.245	5.24	9.53×10^{-2}	7.08	8.40	0.18

Table 3 Magnetic and dielectric properties for FRAs [experimental (Exp.) and simulated (Sim.) values]

Sample	ϵ'_r	tg δ_E	tg δ_M	μ'_r	Maximum resistance (Ω)		Resistance in the f_0 (Ω)	
					Exp.	Sim.	Exp.	Sim.
GdIG	14.09	2.5×10^{-2}	2.8×10^{-4}	1.10	105.51	99.54	59.57	50.00
GdIG _{0.75} YIG _{0.25}	10.87	4.0×10^{-4}	2.5×10^{-4}	1.00	117.72	123.35	50.00	50.16
GdIG _{0.5} YIG _{0.5}	9.43	3.5×10^{-3}	3.5×10^{-4}	0.90	130.15	138.07	48.55	46.23
GdIG _{0.25} YIG _{0.75}	–	2.1×10^{-3}	2.5×10^{-4}	–	144.40	–	50.02	–
YIG	20.00	1.4×10^{-3}	2.5×10^{-4}	0.35	171.23	331.39	46.75	46.16

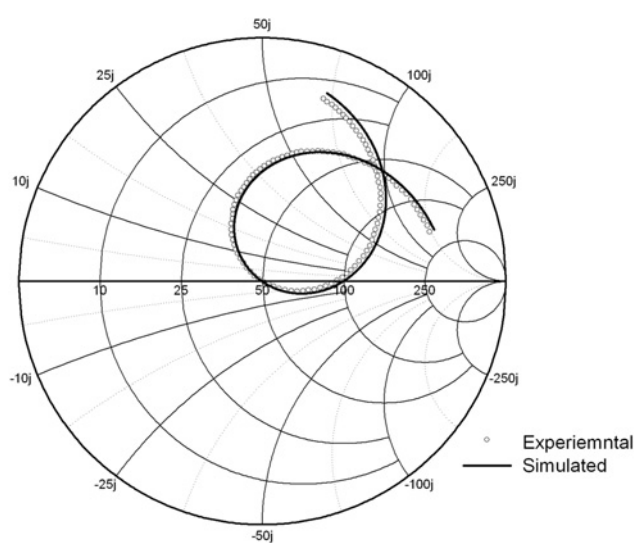


Figure 6 Experimental (measured) and theoretical (simulated) input impedance (Smith chart) of GdIG_{0.75}YIG_{0.25} FRA

and YIG (-283.82 ppm/ $^{\circ}$ C). All FRAs presented a low negative value, which symbolise suitable results for microwave applications such as mobile communication systems or satellite broadcast systems.

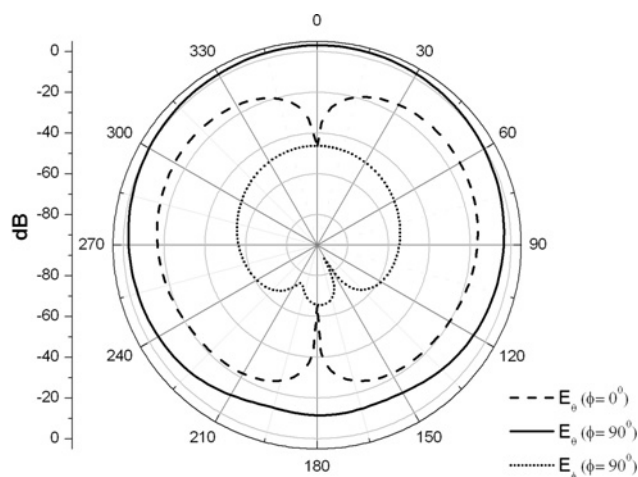


Figure 8 Theoretical radiation patterns of the GdIG_{0.75}YIG_{0.25} FRA

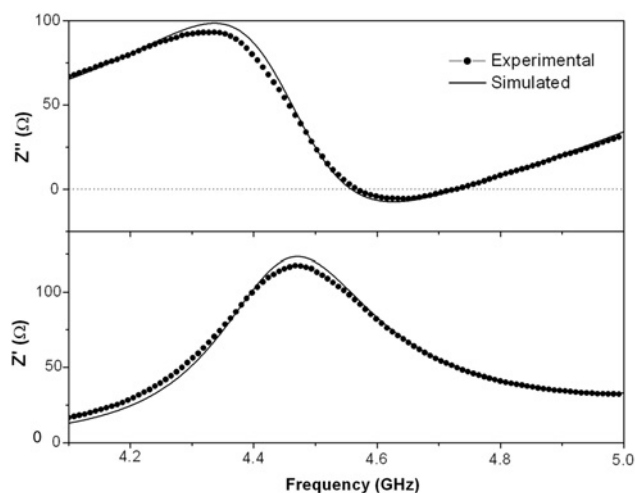


Figure 7 Experimental and simulated input impedance of GdIG_{0.75}YIG_{0.25} FRA

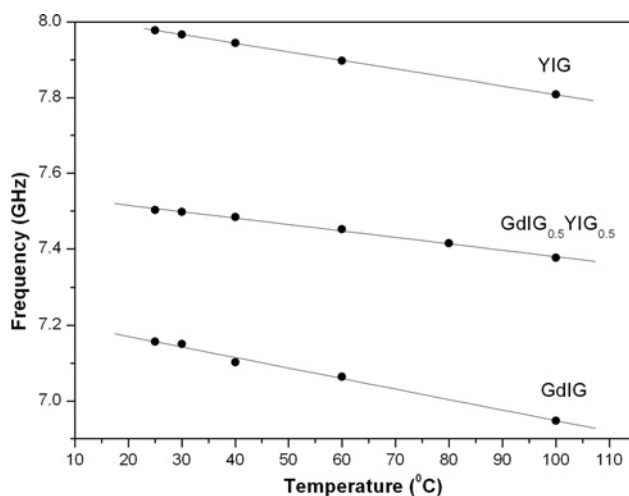


Figure 9 Linear fit with the experimental points used to calculate coefficient of resonant frequency (τ_f) for GdIG, GdIG_{0.5}YIG_{0.5} and YIG

4 Conclusion

In this paper, we did a study on the microwave properties of a ferrimagnetic ceramic composite ($\text{Gd}_3\text{Fe}_5\text{O}_{12}$) $\text{GdIG}_X\text{-YIG}_{1-X}$ ($\text{Y}_3\text{Fe}_5\text{O}_{12}$). The magnetic and dielectric measurements at microwaves frequency were made through the Hakki–Coleman's procedure and through the excitation of a cylindrical FRA. The hysteresis loops of the $\text{GdIG}_X\text{YIG}_{1-X}$ ferrimagnetic composite were obtained.

The numerical simulation study was performed using Ansoft's HFSSTM software. The agreement between the experimental data and the simulated results is very good. These results showed that the ferrimagnetic composite $\text{GdIG}_X\text{YIG}_{1-X}$ could operate as a magneto-dielectric antenna with bandwidth in the range of 7.5–11%, in the frequency range of 4.4–5.3 GHz, only changing the composition of the resonator. Additionally, all FRAs presented a low positive value of τ_f , which symbolises suitable results for microwave applications such as mobile communication systems or satellite broadcast systems.

5 Acknowledgments

This work was partly sponsored by CAPES, CNPq and FUNCAP (Brazilian agencies), CELESTICA, the US Air Force Office of Scientific Research (AFOSR) (FA9550-08-1-0210 and FA9550-07-1-0040), and by the Millennium Science Nucleus Basic and Applied Magnetism P06-022F and Fondecyt 1080164 (Chile).

6 References

- [1] MOULSON A.J., HERBERT J.M.: 'Electroceramics: materials–properties–applications' (John Wiley & Sons Inc, 2003, 2nd edn.), p. 300
- [2] LUK K.-M., LEUNG K.-W.: 'Dielectric resonator antennas' (Research Studies Press, 2003, 1st edn.)
- [3] PENG Z., WANG H., YAO X.: 'Dielectric resonator antennas using high permittivity ceramics', *Ceram. Int.*, 2004, **30**, pp. 1211–1214
- [4] POZAR D.M.: 'Microwave engineering' (John Wiley & Sons Inc., 1998, 2nd edn.), p. 665
- [5] WU Z., DAVIS L.E., DROSSOS G.: 'Cylindrical dielectric resonator antenna arrays'. 11th Int. Conf. Antennas and Propagation, Conference Publication no. 480, 2001, pp. 668–671
- [6] FECHINE P.B.A., DA ROCHA M.J.S., SANTOS M.R.P., ET AL.: 'Microstructural and electrical properties of PbTiO_3 screen-printed thick films', *J. Mater. Sci.: Mater. Electron.*, 2008, **19**, pp. 973–980
- [7] FECHINE P.B.A., ALMEIDA A.F.L., FREIRE F.N.A., ET AL.: 'Dielectric relaxation of BaTiO_3 (BTO)- $\text{CaCu}_3\text{Ti}_4\text{O}_{12}$ (CCTO) composite screen-printed thick films at low temperatures', *Mater. Chem. Phys.*, 2006, **96**, pp. 402–408
- [8] ALMEIDA A.F.L., FECHINE P.B.A., GÓES J.C., ET AL.: 'Dielectric properties of BaTiO_3 (BTO)- $\text{CaCu}_3\text{Ti}_4\text{O}_{12}$ (CCTO) composite screen-printed thick films for high dielectric constant devices in the medium frequency (MF) range', *Mater. Sci. Eng. B*, 2004, **111**, pp. 113–123
- [9] ALMEIDA A.F.L., FECHINE P.B.A., SASAKI J.M., ET AL.: 'Optical and electrical properties of barium titanate-hydroxyapatite composite screen-printed thick films', *Solid State Sci.*, 2004, **6**, pp. 267–278
- [10] FECHINE P.B.A., TÁVORA A., KRETLY L.C., ET AL.: 'Microstrip antenna on a high dielectric constant substrate: BaTiO_3 (BTO)- $\text{CaCu}_3\text{Ti}_4\text{O}_{12}$ (CCTO) composite screen-printed thick films', *IEEE J. Electron. Mater.*, 2006, **35**, (10), pp. 1848–1856
- [11] ALMEIDA A.F.L., FECHINE P.B.A., KRETLY L.C., SOMBRA A.S.B.: ' BaTiO_3 (BTO)- $\text{CaCu}_3\text{Ti}_4\text{O}_{12}$ (CCTO) substrates for microwave devices and antennas', *J. Mater. Sci.*, 2006, **41**, (14), pp. 4623–4631
- [12] SABOIA K.D.A., FECHINE P.B.A., SANTOS M.R.P., ET AL.: 'Composite screen-printed thick films for high dielectric constant devices: $\text{Bi}_4\text{Ti}_3\text{O}_{12}$ - $\text{CaCu}_3\text{Ti}_4\text{O}_{12}$ films', *Polym. Compos.*, 2007, **28**, (6), pp. 771–777
- [13] PLOURDE J.K., LINN D.F., O'BRYAN H.M.J., THOMSON JR. J.: ' $\text{Ba}_2\text{Ti}_9\text{O}_{20}$ as a microwave dielectric resonator', *J. Am. Ceram. Soc.*, 1975, **58**, (9–10), pp. 418–420
- [14] GOLDMAN A.: 'Magnetic ceramics (ferrites)', in 'Engineered Materials Handbook – Ceramics and Glasses', vol. 4 (ASM International – The Materials Information Society, 1991), p. 1161
- [15] NENASHEVA E.A., KARTENKO N.F.: 'High dielectric constant microwave ceramics', *J. Eur. Ceram. Soc.*, 2001, **21**, pp. 2697–2701
- [16] HAKKI B.W., COLEMAN P.D.: 'A dielectric resonator method of measuring inductive capacities in the millimeter range', *IRE Trans. Microw. Theory Tech.*, 1960, **8**, (4), pp. 402–410
- [17] KOBAYASHI Y., KATOH M.: 'Microwave measurement of dielectric-properties of low-loss materials by the dielectric rod resonator method', *IEEE Trans. Microw. Theory Tech.*, 1985, **MTT-33**, (7), pp. 586–592

- [18] GRABOVICKIC R.: 'Accurate calculations of geometrical factors of Hakki-Coleman shielded dielectric resonators', *IEEE Trans. Appl. Supercond.*, 1999, **9**, (3), pp. 4607–4612
- [19] CASTRO P.J., NONO M.C.A.: 'Microwave properties of barium nanotitanate dielectric resonators', *J. Microw. Optoelectron.*, 1999, **1**, (4), pp. 12–19
- [20] LONG S.A., MCALLISTER M.W., SHEN L.C.: 'The resonant cylindrical dielectric cavity antenna', *IEEE Trans. Antennas Propag.*, 1983, **AP-31**, (3), p. 406
- [21] KAJFEZ D., GUILLON P.: 'Dielectric resonators' (The Artech House Microwave Library, 1986)
- [22] JUNKER G.P., KISHK A.A., GLISSON A.W., KAJFEZ D.: 'Effect of air-gap on cylindrical dielectric resonator antenna operating in TM(01) mode', *Electron. Lett.*, 1994, **30**, (2), pp. 97–98
- [23] JUNKER G.P., KISHK A.A., GLISSON A.W., KAJFEZ D.: 'Effect of an air-gap around the coaxial probe exciting a cylindrical dielectric resonator antenna', *Electron. Lett.*, 1994, **30**, (3), pp. 177–178
- [24] SÁNCHEZ R.D., RIVAS J., VAQUEIRO P., LOPEZ-QUINTELA M.A., CAEIRO D.: 'Particle size effects on magnetic garnets prepared by a properties of yttrium iron sol-gel method', *J. Magn. Magn. Mater.*, 2002, **247**, pp. 92–98
- [25] ALMEIDA A.F.L., SILVA R.R., ROCHA H.H.B., ET AL.: 'Experimental and numerical investigation of a ceramic dielectric resonator (DRA): $\text{CaCu}_3\text{Ti}_4\text{O}_{12}$ (CCTO)', *Phys. B: Condens. Matter*, 2008, **403**, (1), pp. 586–594
- [26] BALANIS C.A.: 'Antenna theory: analysis and design' (John Wiley & Sons, Inc., New York, 1997, 2nd edn.)